



## Article

# Research on Modification of Oxygen-Producing Adsorbents for High-Altitude and Low-Pressure Environments

Ye Li <sup>1,2</sup> , Huiqing Yue <sup>1</sup>, Quanli Zhang <sup>2,\*</sup>, Dumin Yan <sup>3,4</sup>, Ziyi Li <sup>1</sup>, Zhiwei Liu <sup>1,\*</sup>, Yingshu Liu <sup>1,2</sup>, Yongyan Wang <sup>1</sup>, Shifeng Wang <sup>5</sup> and Xiong Yang <sup>1,5,\*</sup> 

<sup>1</sup> School of Energy and Environmental Engineering, University of Science and Technology Beijing, Beijing 100083, China; 17863907749@163.com (Y.L.); yhq23345@163.com (H.Y.); ziyili@ustb.edu.cn (Z.L.); yslu@ustb.edu.cn (Y.L.); 13408454472@163.com (Y.W.)

<sup>2</sup> Songshan Lake Materials Laboratory, Dongguan 523000, China

<sup>3</sup> School of Earth Science and Engineering, Nanjing University, Nanjing 210008, China; ydm111222@sina.com

<sup>4</sup> Tibet Headquarters, China Railway Construction Engineering Group, Lhasa 850000, China

<sup>5</sup> Key Laboratory of Plateau Oxygen and Living Environment of Tibet Autonomous Region, College of Science, Tibet University, Lhasa 850000, China; wsf@utibet.edu.cn

\* Correspondence: zhangquanli@sslalab.org.cn (Q.Z.); liuzhiwei@ustb.edu.cn (Z.L.); yangx@ustb.edu.cn (X.Y.)

**Abstract:** In oxygen production on plateaus, pressure swing adsorption (PSA) oxygen production is currently the most commonly used oxygen production method. In plateau regions, low pressure leads to a decrease in adsorbent nitrogen–oxygen separation performance, which affects the performance of PSA oxygen production, so it is particularly important to enhance adsorbent nitrogen–oxygen separation performance. In this paper, Li-LSX (lithium low-silicon aluminum X zeolite molecular sieve) adsorbents were modified using the liquid phase ion exchange method, and five kinds of modified adsorbents were obtained, namely AgLi-LSX, CaLi-LSX, ZnLi-LSX, CuLi-LSX, and FeLi-LSX, respectively. The influences of different metal ions and modification time lengths on the adsorbent nitrogen adsorption and nitrogen–oxygen separation coefficients were analyzed. Through theoretical calculations, the nitrogen and oxygen adsorption and separation performances of the modified adsorbents at different altitudes and low adsorption pressures were investigated. It is shown that the nitrogen adsorption capacity of the AgLi-LSX-1 adsorbent obtained from the modification experiment reaches 27.92 mL/g, which is 3.24 mL/g higher than that of Li-LSX; the nitrogen–oxygen separation coefficients of S1 and S2 are 19.24 and 7.54 higher, respectively; and the nitrogen–oxygen separation coefficients of S4 are 20.85 and 7.54 higher than those of Li-LSX, respectively. With the increase in altitude from 50 m to 5000 m, the nitrogen–oxygen separation coefficient of the AgLi-LSX-1 adsorbent increased rapidly from 20.85 to 57, and its nitrogen–oxygen separation coefficient S4 exceeded that of the Li-LSX adsorbent to reach 47.61 at an altitude of 4000 m. Therefore, the modified adsorbent AgLi-LSX-1 in this paper can enhance the performance of the PSA oxygen process for oxygen production in plateau applications.

**Keywords:** plateau low-pressure environment; PSA oxygen production process; adsorbent; metal ion modification; nitrogen–oxygen separation



check for updates

**Citation:** Li, Y.; Yue, H.; Zhang, Q.; Yan, D.; Li, Z.; Liu, Z.; Liu, Y.; Wang, Y.; Wang, S.; Yang, X. Research on Modification of Oxygen-Producing Adsorbents for High-Altitude and Low-Pressure Environments.

*Inorganics* **2024**, *12*, 250. <https://doi.org/10.3390/inorganics12090250>

Academic Editor: Elsa Lasseguette

Received: 10 July 2024

Revised: 12 August 2024

Accepted: 15 August 2024

Published: 14 September 2024



**Copyright:** © 2024 by the authors. Licensee MDPI, Basel, Switzerland. This article is an open access article distributed under the terms and conditions of the Creative Commons Attribution (CC BY) license (<https://creativecommons.org/licenses/by/4.0/>).

## 1. Introduction

A plateau region is characterized by thin air, low air pressure, and other characteristics that often result in hypoxia, triggering shortness of breath and other issues. To promote the construction of the plateau region and the promotion of high-quality economic development, solving the problem of hypoxia in the plateau region is the key. The most direct and effective way to address the problem of plateau oxygen deficiency is to supply oxygen to the plateau. Pressure-variable adsorption (PSA) oxygen technology has been expanding its industrial applications with unique advantages and is widely used in plateau environments. One of the keys to determining the high oxygen production performance of

the plateau PSA oxygen generation process in a plateau low-pressure environment is the use of oxygen adsorbents with high oxygen and nitrogen separation coefficients. At present, most of the A-type and X-type adsorbents are used in the plateau PSA oxygen generation process in the industry; however, in the high-altitude and low-pressure environments of this adsorbent, the N<sub>2</sub> adsorption capacity and nitrogen and oxygen separation coefficients will be greatly reduced, which will affect the oxygen production performance of oxygen generating devices. Therefore, the development of a high-performance oxygen adsorbent with plateau adaptability is the key to ensuring the oxygen production performance of the oxygen generation process in a low-pressure plateau environment [1].

Li-LSX has a greater nitrogen adsorption capacity and nitrogen–oxygen separation capacity than ordinary X zeolite [2–4]. The metal ion modification on the basis of Li-LSX is considered to be the most effective way to further improve the separation performance of adsorbents. Charles G. Coe [5] and Kirner et al. [6] concluded that the exchange degree of Li<sup>+</sup> must be greater than 70% for its N<sub>2</sub> adsorption capacity to increase rapidly. R.T. Yang et al. [4] obtained a Li-Ag-X adsorbent by exchanging Li<sup>+</sup> and Ag<sup>+</sup> for an X-type adsorbent with low silica–aluminum ratios, and its oxygen–nitrogen separation factor can reach over 6.0. Oka et al. [7] introduced Ca<sup>2+</sup> into a Li-LSX adsorbent and identified that the presence of Ca<sup>2+</sup> has an effect on the position of Li<sup>+</sup> in the skeletal structure, which affects the gas adsorption separation performance of the adsorbent. Fu [8] obtained the adsorption isotherms of N<sub>2</sub> and O<sub>2</sub> by 5A and Li-LSX zeolites at 0–300 kPa by simulation. With the decrease in temperature and the increase in pressure, the adsorption of both N<sub>2</sub> and O<sub>2</sub> at high pressure showed an increasing trend, which shows that the temperature difference in the plateau environment has a significant effect on the adsorption process. Previous studies on the metal ion modification of adsorbents for nitrogen–oxygen separation have been abundant, but there are few reports on the targeted modification and screening of Li-LSX for the special environment found on plateaus. In order to better utilize the PSA oxygen generation process in production, the development of a new oxygen adsorbent with high N<sub>2</sub> adsorption capacity and high nitrogen and oxygen separation coefficient under the low-pressure environment conditions of a plateau is an important research and development direction to enhance the performance of the PSA oxygen generation process for oxygen production on plateaus.

In molecular sieve adsorption, the skeleton structure is used to provide a large specific surface area, and different coordination cations can change the pore size distribution, the specific surface area in the pore and the electric field in the crystal, thus changing the adsorption performance of the molecular sieve [9]. In this paper, we will carry out the modification experiments of the Li-LSX adsorbent with five different metal ions (Ag<sup>+</sup>, Ca<sup>2+</sup>, Zn<sup>2+</sup>, Cu<sup>2+</sup>, and Fe<sup>3+</sup>), using the liquid-phase ion exchange method, and analyze the influence of different modification duration on its nitrogen–oxygen adsorption and nitrogen–oxygen separation coefficients. We will test the specific surface and pore-size distributions of the modified adsorbent and study the influence of the modified adsorbent loaded with metal cation species as well as its surface area and pore-size distributions on its nitrogen–oxygen adsorption and separation performance. This could guide the metal ion modification of a molecular sieve suitable for PSA oxygen production in a plateau area. Finally, the adsorption and separation performances of the modified adsorbents in a low-adsorption pressure range at different altitudes were compared by theoretical calculation so as to select the high-performance adsorbents most suitable for high-altitude and low-pressure conditions.

## 2. Experimental Section

### 2.1. Materials

A commercial X-type zeolite with a Si/Al ratio of 1 (Linde Li-LSX, lot 945084060002), as well as calcium nitrate (Ca(NO<sub>3</sub>)<sub>2</sub>, 99.9%), Beijing HongHu LianHe HuaGong ChanPin Co., Ltd., Beijing, China; silver nitrate (Ag(NO<sub>3</sub>)<sub>3</sub>, 99.99%), Beijing HongHu LianHe HuaGong ChanPin Co., Ltd., Beijing, China; copper nitrate (Cu(NO<sub>3</sub>)<sub>2</sub>·3H<sub>2</sub>O, 99.9%), Shanghai Al-

addin Biochemical Technology Co., Ltd., Shanghai, China; zinc acetate ( $\text{Zn}(\text{CH}_3\text{COO})_2 \cdot 2\text{H}_2\text{O}$ , 99.9%), Shanghai Aladdin Biochemical Technology Co., Ltd., Shanghai, China; ferric nitrate ( $\text{H}_{18}\text{FeN}_3\text{O}_{18}$ , 99.9%), Shanghai Aladdin Biochemical Technology Co., Ltd., Shanghai, China; and deionized water, was used in the preparation of the ion-exchange solutions.

## 2.2. Preparation of Sorbents

For each metal ion modification experiment, different metal salt solutions of 0.05 mol/L were configured. Four control groups were established, and round-bottomed flasks containing the same metal salt solution and Li-LSX raw powder were immersed in an oil bath for dynamic ion exchange at 100 °C. The modification times were 0.5 h, 1.0 h, 1.5 h, and 2.0 h. After dynamic ion exchange, centrifugation separated the bottom samples. These samples were transferred to 500 mL beakers (with a rotor), and 300 mL of deionized water was added. Using a magnetic stirrer, the samples were cleaned for 10 minutes, repeating the process six times. Filtration yielded a cleaned filter cake, which was then dried in an oven at 28 °C for 48 h.

Through the above experimental steps of metal ion modification, five modified samples were obtained, named AgLi-LSX, CaLi-LSX, ZnLi-LSX, CuLi-LSX and FeLi-LSX, and numbered 1, 2, 3 and 4 according to the modification times of 0.5 h, 1.0 h, 1.5 h and 2.0 h, respectively, the modification times of 0.5 h, 1.0 h, 1.5 h and 2.0 h were named “AgLi-LSX-1”, “AgLi-LSX-2”, “AgLi-LSX-3” and “AgLi-LSX-4”. As shown in Figure 1, the nominating rule of the adsorbent in this paper is that different modified cations are placed before the name of the adsorbent, and the modification time of the same modified cationic adsorbent is represented by the number after the name of the adsorbent.



**Figure 1.** Naming rules for modified adsorbents.

The separation coefficients obtained by four methods are S1, S2, S3, and S4.

## 2.3. Nitrogen and Oxygen Adsorption Performance Analysis

In the practical application of PSA air separation for oxygen production, the main components of adsorption bed gas are  $\text{N}_2$ ,  $\text{O}_2$ , and Ar [10]. Given the similar adsorption properties of  $\text{O}_2$  and Ar, the evaluation of the adsorbent’s separation performance focuses on nitrogen and oxygen. The Autosorb-iQ adsorption instrument was used to determine the modified adsorbent’s nitrogen and oxygen adsorption isotherms. Subsequently, the isotherm of nitrogen and oxygen were tested at 25 °C (0~101.3 kPa), and the separation coefficient was calculated. The specific surface area and pore size distribution of the modified adsorbent were tested using the Autosorb-iQ instrument under the same degassing parameters (vacuum degassing at 350 °C for 8 h, heating rate 2 °C/min). The pore size distribution was calculated from the NLDFT (Non-Local Density Functional Theory) model of Ar@77K-Zeolites. The pore volume was calculated by the adsorption capacity of  $P/P_0 = 0.99$ , and the  $S_{\text{BET}}$  (specific surface area) was determined within the  $P/P_0$  range of 0.05~0.25 using the BET method.

The nitrogen–oxygen separation coefficients were calculated using the following four calculations, the separation coefficient S1 was calculated as the ratio of nitrogen–oxygen adsorption, and the separation coefficient S2 was calculated by fitting the Langmuir equation [11]. For PSA method, S2 is usually used to judge the separation performance of the adsorbent, and the better the separation performance, the higher the S2 value. The separation coefficient S3 is calculated by the IAST (Ideal Adsorption Solution Theory)

model, which is based on the adsorption equilibrium data of one component and is used to predict the equilibrium data of binary mixtures or even multi-component mixtures. In contrast to the first three separation coefficients, which do not consider the process parameters of the PSA process, this paper introduces the parameter S4. S4 accounts for the adsorption and desorption pressures in the PSA process. Specifically, S4 is calculated as the ratio of the difference between the adsorbed capacity of nitrogen and oxygen gases at the highest adsorption pressure and the lowest desorption pressure, multiplied by S2 [11].

### 3. Results and Discussion

#### 3.1. Specific Surface Area and Pore Size Analysis of Modified Adsorbents

The increase in specific surface area and pore volume of the modified adsorbent compared to the original powder Li-LSX is due to the use of multivalent metal cations that can replace multiple monovalent  $\text{Li}^+$ , thus leading to an increase in specific surface area and pore volume of the adsorbent. The large increase in both specific surface area and pore volume of the adsorbent by the introduction of metal ions is due to the modification of the pore channels during the introduction of metal ions.

#### 3.2. Pore Size Distribution Analysis

The adsorption capacity of an adsorbent is related to the pore size of the material, which is an important physical parameter of the adsorbent [12]. In general, at low pressure, the microporous pore size is about two times the kinetic diameter of the gas molecule, when it plays a major role in adsorption. Therefore, the highest value of pore volume per unit pore diameter within the range of 2 times 0.728 nm of the molecular dynamics diameter of  $\text{N}_2$  was taken for comparative analysis, and it can be concluded from the highest value of pore volume per unit pore diameter of different adsorbents,  $dV$ , that the adsorbent modified with  $\text{Ag}^+$  and  $\text{Ca}^{2+}$  has a significant increase in pore volume per unit pore diameter,  $dV$ , in comparison to that of the original powder Li-LSX. In addition to the obvious changes in the specific surface area and pore size of the adsorbent after modification by metal ions, the nature of the cations after exchange also affects or even determines the adsorption performance of the molecular sieves. The change in pore size is also due to the modification of the original structure by metal ions, and  $\text{Ag}^+$  has a stronger adsorption effect due to the formation of large  $\pi$  bonds by complexation [13].

#### 3.3. Study of Nitrogen–Oxygen Separation Performance of Modified Adsorbent

As shown in Figure 2, X-type oxygen adsorbents with structures such as supercages, square nanocages and hexagonal prisms in the unit cell and cations can be located in five positions such as SI, SI', SII, SII' and SIII [14]. SI is located in the center of the hexagonal prism, SI' is located in the six-membered ring structure, SII is located in the supercage near the six-membered ring, SII' is located in the octahedral cage, and SIII is located in the supercage near the four-membered ring. The distribution of cations outside the skeleton is influenced by both pore size and electrostatic repulsion. As a result, metal ions outside the skeleton may be present only in specific locations rather than uniformly throughout [15].

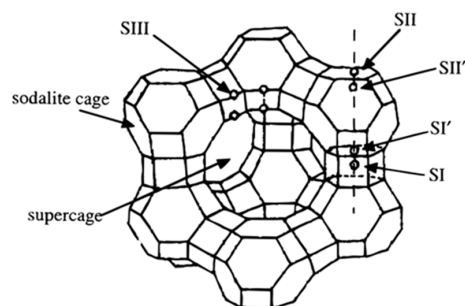


**Figure 2.** Schematic diagram of the distribution of cations outside the skeleton of X-type oxygen-producing adsorbent.

The nitrogen and oxygen adsorption isotherm of AgLi-LSX modified adsorbent is shown in Figure 3 and the nitrogen and oxygen separation performance of AgLi-LSX is shown in Table 1. After the ion-modified molecular sieve, Ag<sup>+</sup> is introduced into the molecular sieve. The exchange of silver ions to non-skeleton lithium ions changes the cation. The change in cation is related to the pore structure and surface electrical properties of the molecular sieve and ultimately affects the adsorption and separation performance, and Ag ions can form weak  $\pi$  bond adsorption with nitrogen. As shown in Figure 3, the adsorption isotherms of N<sub>2</sub> and O<sub>2</sub> of AgLi-LSX adsorbent conform to the law of the adsorption model, and the partial isotherm of type I shows that at constant temperature, the adsorption capacities of N<sub>2</sub> and O<sub>2</sub> are a single function of pressure. With the increase in modification time, the adsorption capacity of N<sub>2</sub> and O<sub>2</sub>, especially N<sub>2</sub>, decreased gradually. The N<sub>2</sub> adsorption capacity of AgLi-LSX adsorbent decreased from 27.92 mL/g to 10.32 mL/g, and the N<sub>2</sub> and O<sub>2</sub> separation coefficients S1, S2, and S3 decreased from 6.12 to 3.55, from 30.82 to 10.24 and from 18.77 to 6.92, respectively. This is because the introduction of a small amount of Ag<sup>+</sup> can be well loaded on the SII site of the adsorption site and form a strong electric field of silver clusters, which enhances the interaction with nitrogen and oxygen molecules [16]. At the same time, due to the large radius of Ag<sup>+</sup>, the SII position can produce a strong interaction force with N<sub>2</sub> molecules, thus increasing the number of effective adsorption sites of the adsorbent (due to the small radius of Li<sup>+</sup>, the SII position can not adsorb N<sub>2</sub>). Therefore, the nitrogen and oxygen adsorption capacity of AgLi-LSX-1 is increased compared with that of Li-LSX. As the increase in the adsorption capacity of O<sub>2</sub> is more significant than that of N<sub>2</sub>, the nitrogen and oxygen separation coefficient S1 of AgLi-LSX-1 is slightly decreased compared with that of Li-LSX. The N<sub>2</sub> adsorption capacity and nitrogen and oxygen separation coefficients S2 and S3 of AgLi-LSX-2, AgLi-LSX-3, and AgLi-LSX-4 showed a gradually decreasing trend. In particular, the decreasing trend of AgLi-LSX-3 and AgLi-LSX-4 is more obvious, which may be related to the larger radius of Ag<sup>+</sup> compared with Li<sup>+</sup> and the formation of bank clusters, which lead to the decrease in specific surface area and pore volume of AgLi-LSX-3 and AgLi-LSX-4 [17].

**Table 1.** Nitrogen and oxygen separation performance of AgLi-LSX and CaLi-LSX adsorbent.

Adsorbent	Adsorption Capacity (mL/g)		S1	S2	S3	$q_{mN_2}$	$q_{mO_2}$	$b_{N_2}$	$b_{O_2}$
	N <sub>2</sub>	O <sub>2</sub>							
Li-LSX	24.68	3.48	7.09	11.58	11.23	2.5694	37.788	0.0074	0.00004
AgLi-LSX-1	27.92	4.56	6.12	30.82	18.77	1.5123	3.4369	0.0438	0.0006
AgLi-LSX-2	23.09	3.71	6.22	28.78	18.04	1.2676	2.8760	0.0397	0.0006
AgLi-LSX-3	22.79	4.82	4.73	23.06	10.63	1.2675	203.98	0.0376	0.00001
AgLi-LSX-4	10.32	2.99	3.45	10.24	6.92	0.6360	1.8434	0.0233	0.0008
CaLi-LSX-1	23.11	4.40	5.25	11.18	8.87	2.5607	5.5616	0.0070	0.0003
CaLi-LSX-2	25.83	4.22	6.12	12.21	11.74	2.1566	1.4702	0.0118	0.0016
CaLi-LSX-3	14.94	3.15	4.74	8.23	7.85	1.4178	1.2574	0.0227	0.0020
CaLi-LSX-4	9.13	2.86	3.20	5.15	4.32	1.2269	1.2594	0.0298	0.0013

Note: N<sub>2</sub> and O<sub>2</sub> adsorption were measured at 25 °C and 101 kPa; S1 was calculated as the ratio of nitrogen–oxygen separation coefficients; S2 was calculated as the Langmuir adsorption isotherm fitting parameter; and S3 was derived from the IAST calculation method.

The adsorbent AgLi-LSX-1 obtained by modification for 0.5 h has the best nitrogen and oxygen adsorption separation performance and the highest N<sub>2</sub> adsorption capacity, reaching 27.92 mL/g, which is 13.13% higher than that of the original powder Li-LSX. The nitrogen and oxygen separation coefficients S2 and S3 reached 30.82 and 18.77, respectively. This represents an impressive increase of 166.15% and 67.14%, respectively. The nitrogen and oxygen adsorption separation performance of AgLi-LSX-2 modified for 1.0 h was also improved compared with the original Li-LSX, and the nitrogen and oxygen separation coefficients S2 and S3 increased by 148.53% and 60.64%, respectively. Ag<sup>+</sup> has a stronger adsorption effect due to the complexation to form large  $\pi$  bonds [18], which indicated that

the adsorbent modification scheme developed in this paper had a certain improvement in the enhancement of the nitrogen–oxygen separation performance of the adsorbents.

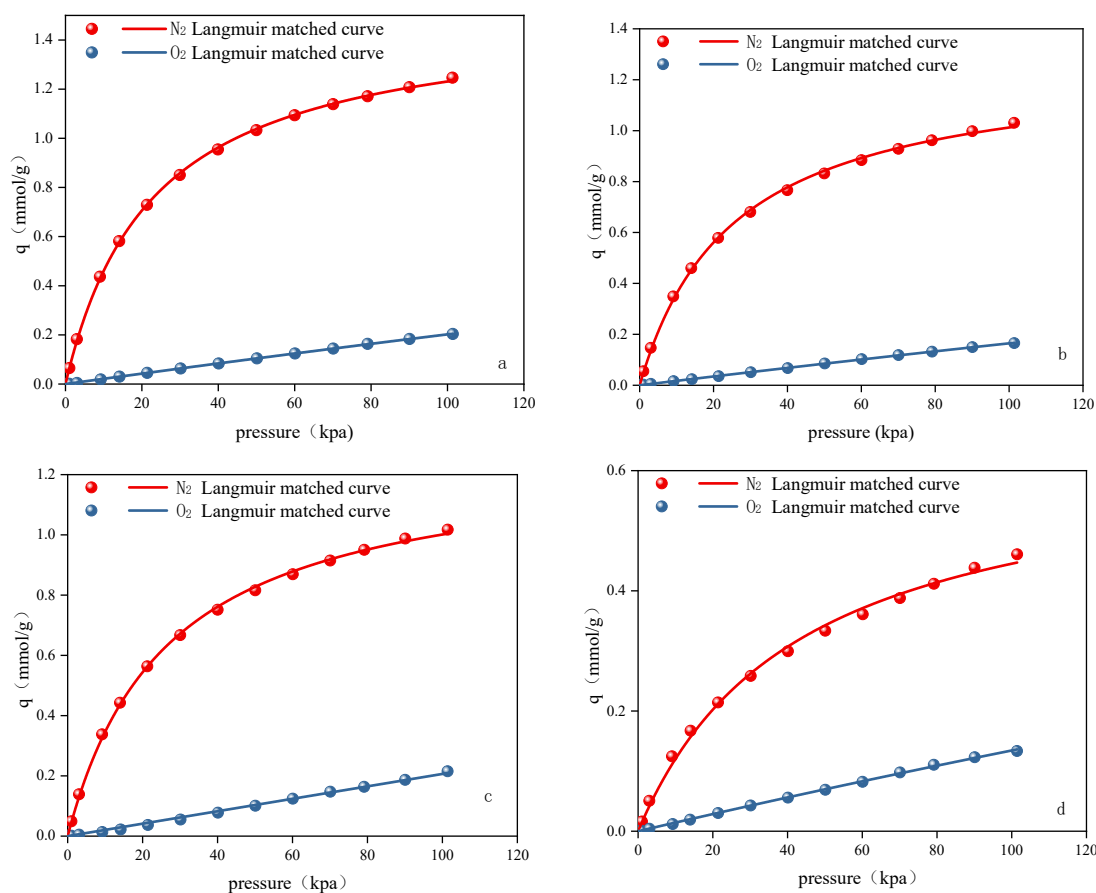


**Figure 3.** AgLi-LSX adsorption isotherms ((a–d) are AgLi-LSX-1, AgLi-LSX-2, AgLi-LSX-3, and AgLi-LSX-4).

As shown in Figure 4, the nitrogen and oxygen adsorption isotherms of CaLi-LSX adsorbent exhibit a gradual increase in adsorption capacity with increasing pressure. Additionally, the adsorption capacities and the separation coefficients of S2 and S3 follow a trend of initially decreasing and increasing with increasing modification time. The  $\text{Ca}^{2+}$  introduced at the modification time of 0.5 h may first exchange part of the  $\text{Li}^+$  in the SIII position. The  $\text{Li}^+$  in this position contributes more to the  $\text{N}_2$  adsorption capacity than  $\text{Ca}^{2+}$ , resulting in a decrease in the number of effective adsorption sites of the adsorbent. Thus, the  $\text{N}_2$  adsorption capacity and nitrogen–oxygen separation coefficients of the obtained CaLi-LSX-1 show a decreasing trend. With the increase in the exchange time to 1.0 h,  $\text{Ca}^{2+}$  began to occupy the SII site. In contrast,  $\text{Li}^+$  in the SII site did not contribute to the  $\text{N}_2$  adsorption, and introducing  $\text{Ca}^{2+}$  could effectively improve the  $\text{N}_2$  adsorption capacity. In this case,  $\text{Ca}^{2+}$  at position SII and  $\text{Li}^+$  at position SIII can contribute to the adsorption simultaneously [19]. The adsorbent's effective adsorption sites were enhanced, so the  $\text{N}_2$  adsorption and nitrogen–oxygen separation coefficient of CaLi-LSX-2 were elevated. When the modification time was increased to 1.5 h and 2.0 h, the  $\text{Ca}^{2+}$  exchange rate continued to rise, and  $\text{Li}^+$  in the SIII position might be completely exchanged by  $\text{Ca}^{2+}$ , leading to reduced interactions between adsorption sites and  $\text{N}_2$ . Consequently, the number of effective adsorption sites decreased. Simultaneously, the large radius of  $\text{Ca}^{2+}$  ions could have diminished the pore volume of the adsorbent, affecting the effective adsorption sites and adsorption performance [20–22]. Therefore, the  $\text{N}_2$  adsorption and nitrogen–oxygen separation coefficients of CaLi-LSX-3 and CaLi-LSX-4 continued to decrease. The pore size

distribution analysis of CaLi-LSX (Figures S5 and S7d) also verified this hypothesis. When the modification time extended from 1.5 h to 2.0 h, the pore volume of micropores showed a decreasing trend.

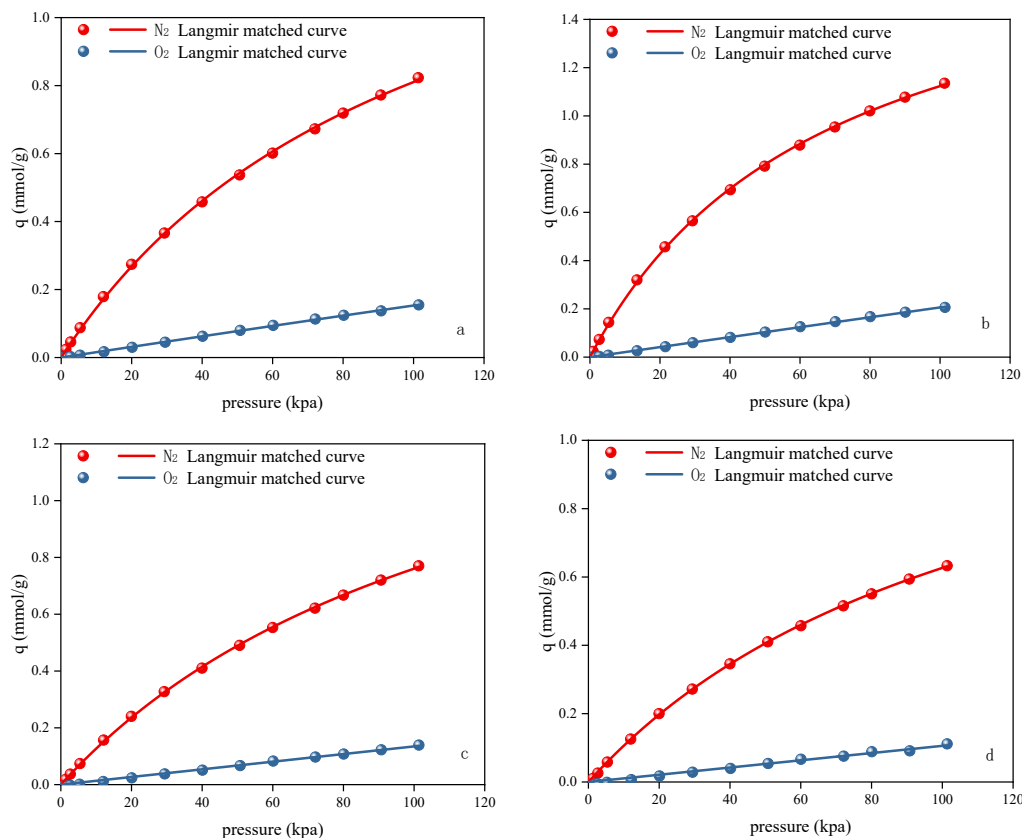


**Figure 4.** CaLi-LSX adsorption isotherms ((a–d) are CaLi-LSX-1, CaLi-LSX-2, CaLi-LSX-3, and CaLi-LSX-4).

The effective adsorption sites of the adsorbent can be improved by using  $\text{Ca}^{2+}$  to modify Li-LSX for 1 h. The CaLi-LSX-2 adsorbent achieved a maximum  $\text{N}_2$  adsorption capacity of 25.83 mL/g, 4.66% higher than the original Li-LSX powder. Additionally, the nitrogen–oxygen separation coefficients of S2 and S3 reached 12.21 and 11.74, respectively, representing improvements of 5.44% and 4.54% compared to the original Li-LSX powder. The nitrogen–oxygen separation coefficients S2 and S3 reached 12.21 and 11.74, respectively, 5.44% and 4.54% higher than those of Li-LSX.

The nitrogen and oxygen adsorption and separation performance of modified ZnLi-LSX were significantly decreased compared with the original powder Li-LSX. It is hypothesized that when the modification time is short, the introduction of  $\text{Zn}^{2+}$  replaces the  $\text{Li}^+$  that can play the role of adsorption on the SIII site, resulting in a decrease in the number of effective adsorption sites of the adsorbent, and at this time, the  $\text{N}_2$  adsorption and nitrogen–oxygen separation coefficients of the modified adsorbent decreased significantly. In addition, the introduction of  $\text{Zn}^{2+}$  may cause the pore plugging phenomenon, which in turn reduces the specific surface area and pore volume of the adsorbent, so the introduction of  $\text{Zn}^{2+}$  not only did not improve the  $\text{N}_2$  adsorption capacity, but also reduced the nitrogen–oxygen adsorption and separation performance of the original powder Li-LSX. The overall adsorption capacities and nitrogen–oxygen separation coefficients of CuLi-LSX and FeLi-LSX were substantially reduced compared with those of the original powder Li-LSX, and it was hypothesized that the introduction of  $\text{Cu}^{2+}$  and  $\text{Fe}^{3+}$  introduction led to the collapse of the adsorbent skeleton. It does not enhance the interaction of the adsorption

sites with nitrogen and oxygen molecules to improve the adsorbent's nitrogen and oxygen separation performance.

### 3.4. Nitrogen and Oxygen Adsorption and Separation Performance of Adsorbent under High Altitude and Low Air Pressure

Considering the nitrogen–oxygen separation coefficient of the oxygen adsorbent in the actual process application, using the ratio of the difference between the adsorbed amount of nitrogen and oxygen bodies at the highest adsorption pressure and the lowest desorption pressure (the final pressure of the desorption process in the PSA process), and multiplying by the nitrogen–oxygen separation coefficient based on the fitting of the Langmuir formula, the nitrogen–oxygen separation coefficient that best meets the process application is obtained as S4. To investigate the performance of the modified adsorbent in the PSA oxygen production process at high altitudes and low air pressure, this section selects an altitude of 5000m (ambient air pressure of 50 kPa) and a pressure fluctuation range of 50–200 kPa for the PSA oxygen production process. Specifically, the final pressure for probe adsorption is set at 200 kPa, and the final pressure for desorption is set at 50 kPa. This pressure condition is used to examine the nitrogen–oxygen separation coefficients of the adsorbents in the AgLi-LSX and CaLi-LSX series.

As shown in Figures 5 and 6, and Table 2, the nitrogen–oxygen adsorption separation performance of the adsorbents obtained using Ag<sup>+</sup> and Ca<sup>2+</sup> at different modification times also differed at high pressures. Among them, the AgLi-LSX-1 adsorbent obtained with a modification time of 0.5 h showed better adsorption performance than the original powder Li-LSX in the high adsorption pressure range (50–200 kPa). The nitrogen–oxygen separation coefficient S4, which can indicate the nitrogen–oxygen adsorption and separation performance of the adsorbent in actual process operation, was increased from 40 to 44 compared with the original powder, which is an improvement of 10%. The nitrogen–oxygen separation coefficients S4 of AgLi-LSX-2 and CaLiLSX-2 decreased from 40 to 35 and from 40 to 25, respectively, with a 12.50% and 37.50% decrease in the nitrogen–oxygen separation coefficient S4 compared to Li-LSX. Therefore, it is concluded that the nitrogen–oxygen adsorption separation performance at an altitude of 5000 m above sea level and a pressure fluctuation range of 50–200 kPa in the PSA oxygen generation process is not as good as that of Li-LSX.

**Table 2.** Comparison of nitrogen and oxygen adsorption separation performance of adsorbents at 5000 m altitude and 200 kPa adsorption pressure.

Adsorbent	Working Capacities (mL/g)		S4
	N <sub>2</sub>	O <sub>2</sub>	
Li-LSX	18.80	5.43	40
AgLiLSX-1	9.31	5.86	44
AgLiLSX-2	6.34	5.07	35
AgLiLSX-3	6.53	6.92	22
AgLiLSX-4	4.06	4.05	10
CaLiLSX-1	13.92	6.15	25
CaLiLSX-2	14.91	6.47	25
CaLiLSX-3	10.56	4.09	21
CaLiLSX-4	7.51	4.02	9

Note: S4 is derived from the calculation of the nitrogen–oxygen partition coefficient for the adsorbent in a process application.

The AgLi-LSX-1 adsorbent with a lower Ag<sup>+</sup> exchange rate has a higher N<sub>2</sub> adsorption capacity, and the Ag<sup>+</sup> complexation still shows better N<sub>2</sub> adsorption performance at high adsorption pressure [23]. It can enhance the oxygen generator's oxygen production performance at high altitudes. With the increase in modification time and Ag<sup>+</sup> exchange rate, the amount of Li<sup>+</sup> replaced on the SIII site gradually increased. Concurrently, the specific surface area and pore volume began to decrease. Consequently, even with increased



adsorption pressure and an enlarged pressure fluctuation range in the PSA process, the nitrogen–oxygen adsorption and separation performances of AgLi-LSX-2, AgLi-LSX-3, and AgLi-LSX-4 adsorbents still could not be improved. Similarly, the CaLi-LSX series adsorbents modified with  $\text{Ca}^{2+}$  are unsuitable for the PSA oxygen generation process at an altitude of 5000 m and a pressure fluctuation range of 50–200 kPa.

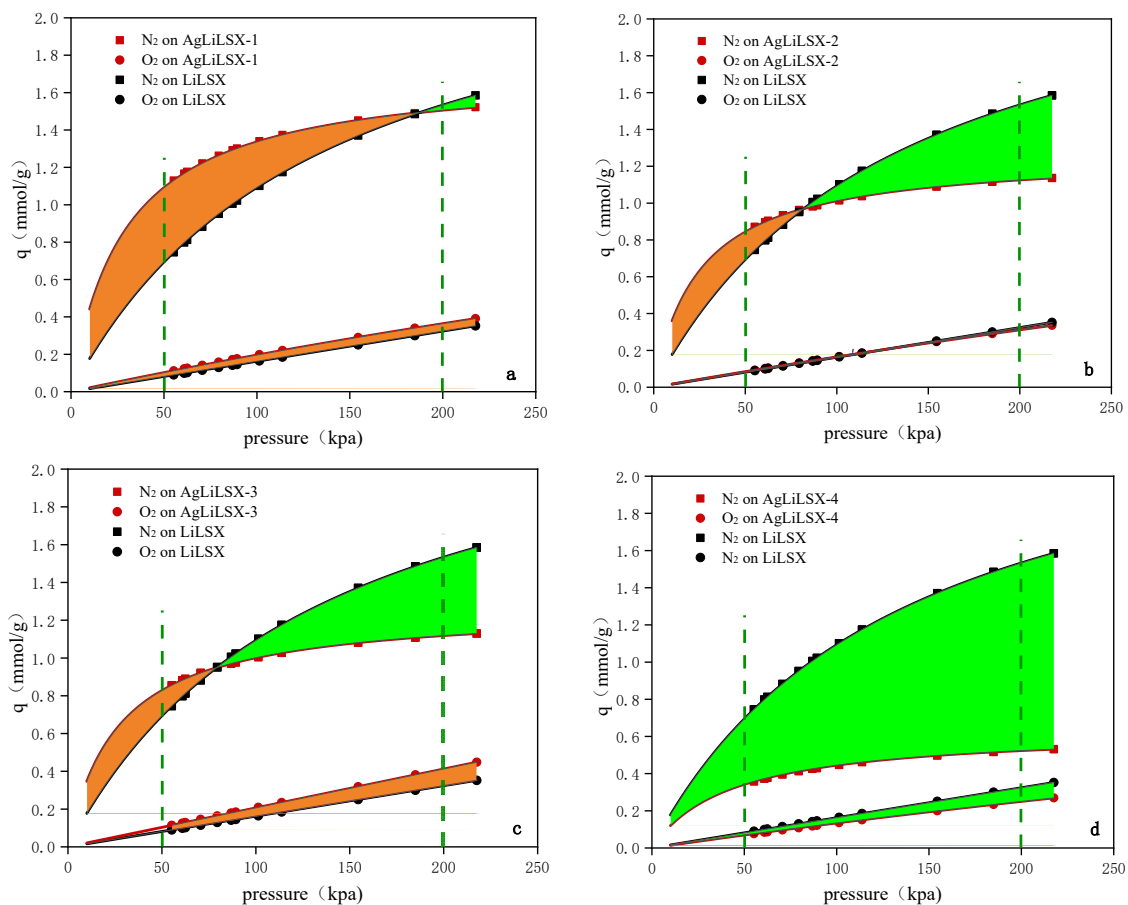


**Figure 5.** AgLi-LSX comparison of nitrogen and oxygen adsorption isotherms of adsorbent and Li-LSX adsorbent under high pressure ((a–d) is AgLi-LSX-1, AgLi-LSX-2, AgLi-LSX-3 and AgLi-LSX-4; BROWN suggests that the adsorption capacity of AgLi-LSX surpasses that of Li-LSX, whereas GREEN indicates the contrary).

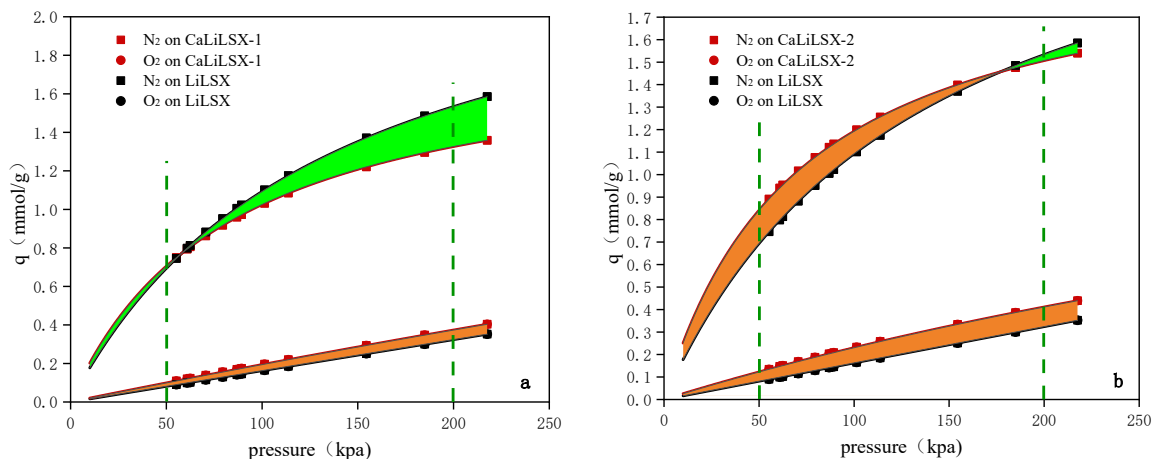


**Figure 6.** Cont.

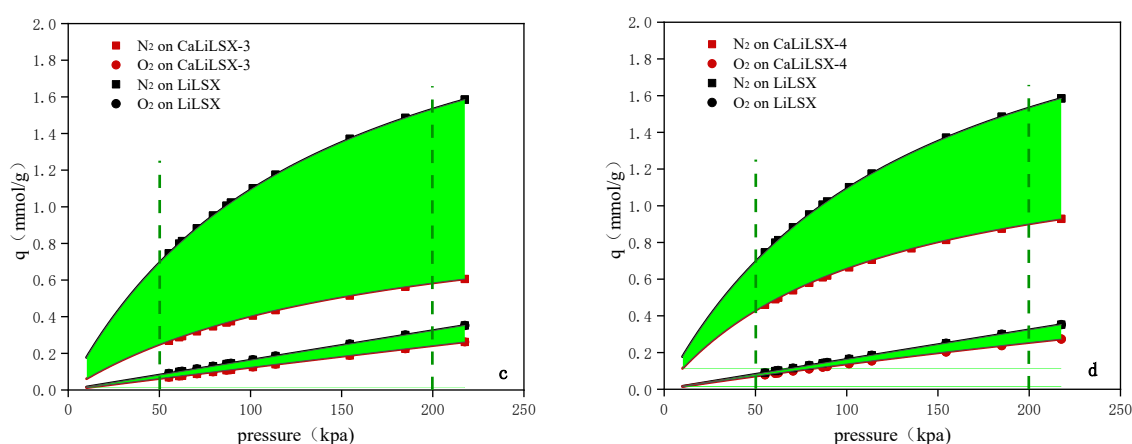


**Figure 6.** CaLi-LSX comparison of nitrogen and oxygen adsorption isotherms of adsorbent and Li-LSX adsorbent under high pressure ((a–d) is CaLi-LSX-1, CaLi-LSX-2, CaLi-LSX-3 and CaLi-LSX-4; BROWN suggests that the adsorption capacity of CaLi-LSX surpasses that of Li-LSX, whereas GREEN indicates the contrary).

Due to the different operating environments, the oxygen plant sometimes operates at different altitudes. The pressure fluctuation range of the PSA oxygen process at different altitudes is also different, so it is necessary to investigate the adsorbent's nitrogen and oxygen adsorption and separation performance under the pressure fluctuation range of the PSA oxygen process at different altitudes. From our previous research, the pressure fluctuation range of the PSA is 101.3–300 kPa at the altitude of 50m, 79–240 kPa at 2000 m, 71–180 kPa at 3000 m, 62–150 kPa at 4000 m, and 55–130 kPa at 5000 m. From this, the nitrogen–oxygen separation coefficients of Li-LSX, AgLi-LSX, and CaLi-LSX adsorbents at different altitudes were calculated and shown in Table 3.

**Table 3.** Comparison of nitrogen and oxygen separation coefficients of adsorbents at different altitudes.

	Altitudes (m)	50	2000	3000	4000	5000
S4	Li-LSX	24.44	31.13	38.53	44.27	49.36
	AgLi-LSX-1	20.85	28.91	38.53	47.61	57.00
	AgLi-LSX-2	16.60	22.78	30.97	38.81	47.02
	CaLi-LSX-1	14.29	18.65	23.59	27.70	31.55
	CaLi-LSX-2	15.26	19.11	23.34	26.91	30.28

Note: S4 is derived from calculating the nitrogen–oxygen separation coefficient for the adsorbent on PSA process application.

When the altitude is above 3000 m, the nitrogen–oxygen separation coefficient S4 of AgLi-LSX-1 gradually starts to higher than that of Li-LSX. With the increase in altitude, the enhancement of S4 is more significant. At 4000 m and 5000 m altitude, the S4 is enhanced by 7.54% and 15.49%, respectively, compared with that of Li-LSX. The higher the altitude, the more significant the enhancement of the nitrogen–oxygen separation coefficient. The higher the altitude, the more significant the enhancement. This is related to the higher total pore volume per unit of material under AgLi-LSX-1 microporous and the stronger interaction force between  $\text{Ag}^+$  and  $\text{N}_2$  molecules at the SII position [16]. The nitrogen–oxygen separation coefficient S4 can indicate the nitrogen–oxygen adsorption and separation performance of the adsorbent in the application of the actual PSA oxygen generation process. Therefore, the AgLi-LSX-1 adsorbent, obtained by  $\text{Ag}^+$  modification, exhibits the strongest nitrogen–oxygen adsorption and separation performance within the low-pressure fluctuation range. It also has the highest recycling efficiency, making it suitable for PSA oxygen generation in high-altitude and low-pressure environments.

#### 4. Future Perspectives

As the core of PSA oxygen production technology, adsorbent determines the process's oxygen production performance and energy consumption. In view of the special conditions in the plateau area, there is no unique oxygen adsorbent, but it is found that the Ag ion-modified Li-LSX adsorbent has potential application value in the plateau low-pressure scene. In future research, we will improve the adsorption and separation performance of the adsorbent under low pressure by changing the cation of the adsorbent. By molding the powder adsorbent into a granular adsorbent and using actual oxygen production experiments, we will establish the adsorbent most suitable for oxygen production in a low-pressure environment, thereby improving oxygen production efficiency in the plateau environment.

#### 5. Conclusions

In this paper, five series of modified adsorbents (AgLi-LSX, CaLi-LSX, ZnLi-LSX, CuLi-LSX and FeLi-LSX) were obtained by using the liquid-phase ion-exchange method to modify the Li-LSX adsorbent with five different metal ions ( $\text{Ag}^+$ ,  $\text{Ca}^{2+}$ ,  $\text{Zn}^{2+}$ ,  $\text{Cu}^{2+}$ , and  $\text{Fe}^{3+}$ ). The nitrogen and oxygen adsorption and separation performance of the five modified adsorbents and the specific surface area, pore volume, and total pore volume of the microporous unit material were also analyzed. The main conclusions are as follows:

(1) The nitrogen and oxygen adsorption and separation performance of AgLi-LSX-1, AgLi-LSX-2 and CaLi-LSX-2 was improved. The nitrogen adsorption capacity of the AgLi-LSX-1 adsorbent reached 27.92 mL/g, and the nitrogen–oxygen separation coefficients S2 and S3 reached 30.82 and 18.77, respectively.

(2) A small amount of  $\text{Ag}^+$  exchange modification of Li-LSX adsorbent can improve the adsorbent's nitrogen–oxygen adsorption and separation performance in the practical PSA oxygen generation process. When the altitude is above 3000 m, the nitrogen–oxygen separation coefficient S4 of AgLi-LSX-1 is gradually higher than that of Li-LSX, and with the increase in altitude, the enhancement of S4 is more significant. At the altitudes of 4000 m and 5000 m, it is enhanced by 7.54% and 15.49%, respectively, compared with that of Li-LSX. The higher the altitude, the more significant the enhancement of the nitrogen–oxygen separation coefficient.

**Supplementary Materials:** The following supporting information can be downloaded at: <https://www.mdpi.com/article/10.3390/inorganics12090250/s1>, Figure S1. Curve of total pore volume of adsorbent with pore width ((a) Li-LSX, (b) AgLi-LSX, (c) CaLi-LSX, (d) ZnLi-LSX, (e) CuLi-LSX, (f) FeLi-LSX). Figure S2. FeLi-LSX adsorption isotherm (a–d is FeLi-LSX-1, FeLi-LSX-2, FeLi-LSX-3, FeLi-LSX-4). Figure S3. CuLi-LSX adsorption isotherm (a–d is CuLi-LSX-1, CuLi-LSX-2, CuLi-LSX-3, CuLi-LSX-4). Figure S4. ZnLi-LSX adsorption isotherm (a–d is ZnLi-LSX-1, ZnLi-LSX-2, ZnLi-LSX-3, ZnLi-LSX-4). Table S1. Agilent ICPOES730 instrument element test. Table S2. Summary of specific surface area and pore volume. Table S3. Maximum pore volume per unit pore diameter of different adsorbents between 0.4–0.728 nm. Table S4. Nitrogen and oxygen separation performance of adsorbent. Figure S5. Specific surface area obtained from CaLi-LSX modification (abcd in order of modification 0.5 h, 1.0 h, 1.5 h and 2.0 h). Figure S6. Specific surface area obtained from AgLi-LSX modification (abcd in order of modification 0.5 h, 1.0 h, 1.5 h and 2.0 h). Figure S7. Pore size distribution and Ar adsorption and desorption of modified adsorbents (a for ZnLi-LSX, b for FeLi-LSX, c for CuLi-LSX, d for CaLi-LSX, e for AgLi-LSX).

**Author Contributions:** Y.L. (Ye Li): Writing—original draft, Writing—review and editing, Methodology, Data curation Investigation; H.Y.: Writing—original draft, Methodology, Data curation; Q.Z.: Conceptualization, Data curation, Writing—review and editing, Investigation; D.Y.: Methodology, Data curation, Formal analysis; Z.L. (Ziyi Li): Supervision, Resources; Z.L. (Zhiwei Liu): Supervision, Validation; Y.L. (Yingshu Liu): Writing—review and editing, Investigation; Y.W.: Writing—review and editing, Validation; S.W.: Investigation, Resources; X.Y.: Validation, Writing—review and editing, Funding acquisition. All authors have read and agreed to the published version of the manuscript.

**Funding:** This research was supported by the NationalKey R&D Program of China (No. 2022YFC3005803) and Tibet Autonomous Region Science and Technology Plan (No. XZ202401YD0004).

**Data Availability Statement:** Data is contained within the article or Supplementary Materials.

**Conflicts of Interest:** The authors declare that they have no known competing financial interests or personal relationships that could have appeared to influence the work reported in this paper.

## References

1. Zhang, Q.; Liu, Y.; Li, Z. Experimental study on oxygen concentrator with wide product flow rate range: Individual parametric effect and process improvement strategy. *Sep. Purif. Technol.* **2021**, *274*, 118918. [[CrossRef](#)]
2. Fu, Y.; Liu, Y.; Li, Z. Insights into adsorption separation of N<sub>2</sub>/O<sub>2</sub> mixture on FAU zeolites under plateau special conditions: A molecular simulation study. *Sep. Purif. Technol.* **2020**, *215*, 117405. [[CrossRef](#)]
3. Baksh, M.S.A.; Kikkinides, E.S.; Yang, R.T. Lithium Type X Zeolite as a Superior Sorbent for Air Separation. *Sep. Sci. Technol.* **1992**, *27*, 277–294. [[CrossRef](#)]
4. Kirner, J.F. Nitrogen Adsorption with Highly Li Exchanged X-Zeolites with Low Si/Al ratio. U.S. Patent 5268023, 17 December 1993.
5. Liu, Y.; Zhang, Q.; Cao, Y. Effect of intermittent purge on O<sub>2</sub> production with rapid pressure swing adsorption technology. *Adsorption* **2020**, *27*, 181–189. [[CrossRef](#)]
6. Coe, C.G.; Kirner, J.F.; Pierantozzi, R.; White, T.R. Nitrogen Adsorption with a Ca and/or Sr Exchanged Lithium X-Zeolite. U.S. Patent US07/811,404, 6 October 1992.
7. Epiepang, F.E.; Yang, X.; Li, J. Air Separation Sorbents: Mixed-Cation Zeolites with Minimum Lithium and Silver. *Chem. Eng. Sci.* **2019**, *198*, 43–51. [[CrossRef](#)]
8. Yang, R.T.; Chen, Y.D.; Peck, J.D.; Chen, N. Zeolites Containing Mixed Cations for Air Separation by Weak Chemisorption-Assisted Adsorption. *Ind. Eng. Chem. Res.* **1996**, *35*, 3093–3099. [[CrossRef](#)]
9. Yang, X.; Epiepang, F.E.; Liu, Y. Heats of adsorption on mixed-cation LiNa-LSX: Estimating SIII site occupancy by Li. *Chem. Eng. Sci.* **2018**, *178*, 194–198. [[CrossRef](#)]
10. Oka, H.; Kasahara, S.; Okada, T.; Yoshida, S.; Harada, A.; Ohki, H.; Okuda, T. Characterization of lithium sites in dehydrated LiCaNaKLSX by 7Li MAS NMR spectroscopy. *Microporous Mesoporous Mater.* **2002**, *51*, 1–5. [[CrossRef](#)]
11. Rege, S.; Yang, R.A. Simple Parameter for Selecting an Adsorbent for Gas Separation by Pressure Swing Adsorption. *Sep. Sci. Technol.* **2001**, *36*, 3355–3365. [[CrossRef](#)]
12. Hutson, N.D.; Rege, S.U.; Yang, R.T. Mixed Cation Zeolites Li-Ag-X as a Superior xy Adsorbent for Air Separation. *AIChE J.* **1999**, *45*, 724–734. [[CrossRef](#)]
13. Panezai, H.; Sun, J.; Jin, X. Influence of alternative cations distribution in AgxLi96-x-LSX on dehydration kinetics and its selective adsorption performance for N<sub>2</sub> and O<sub>2</sub>. *AIP Adv.* **2016**, *6*, 125115. [[CrossRef](#)]
14. Fan, M.; Panezai, H.; Sun, J.; Bai, S.; Wu, X. Thermal and Kinetic Performance of Water Desorption for N<sub>2</sub> Adsorption in Li-LSX Zeolite. *Phys. Chem. C* **2014**, *18*, 23761–23767. [[CrossRef](#)]
15. Ferreira, D.; Magalhães, R.; Bessa, J.; Taveira, P.; Sousa, J.; Whitley, R.D.; Mendes, A. Study of AgLiLSX for Single-Stage High-Purity Oxygen Production. *Ind. Eng. Chem. Res.* **2014**, *53*, 15508–15516. [[CrossRef](#)]
16. Jasra, R.V.; Choudary, N.V.; Bhat, S.G.T. Effect of presorbed water and temperature on adsorption of nitrogen and oxygen in NaCaA and NaMgA zeolites. *Indian J. Chem. Sect. B. Org. Incl. Med.* **1995**, *34*, 15–21. [[CrossRef](#)]
17. Rege, S.U.; Yang, R.T. Limits for Air Separation by Adsorption with LiX Zeolite. *Ind. Eng. Chem. Res.* **1997**, *36*, 5358–5365. [[CrossRef](#)]
18. Jasra, R.V.; Choudary, N.V.; Bhat, S. Correlation of Sorption Behavior of Nitrogen, Oxygen, and Argon with Cation Locations in Zeolite X. *Ind. Eng. Chem. Res.* **1996**, *35*, 4221–4229. [[CrossRef](#)]
19. Fu, Y.; Liu, Y.; Yang, X. Thermodynamic analysis of molecular simulations of N<sub>2</sub> and O<sub>2</sub> adsorption on zeolites under plateau special conditions. *Appl. Surf. Sci.* **2019**, *480*, 868–875. [[CrossRef](#)]
20. Wozniak, A.; Marler, B.; Angermund, K. Water and Cation Distribution in Fully and Partially Hydrated Li-LSX Zeolite. *Chem. Mater. A Publ. Am. Chem. Soc.* **2008**, *20*, 5968–5976. [[CrossRef](#)]
21. Sebastian, J.; Jasra Raksh, V. Anomalous adsorption of nitrogen and argon in silver exchanged zeolite A. *Chem. Commun.* **2003**, *2*, 268–269. [[CrossRef](#)] [[PubMed](#)]
22. Yang, R.T. *Adsorbents: Fundamentals and Applications*; John Wiley & Sons, Inc.: Hoboken, NJ, USA, 2003; pp. 131–156. [[CrossRef](#)]
23. Remy, T.; Peter, S.A.; Van Tendeloo, L. Correction to Adsorption and Separation of CO<sub>2</sub> on KFI Zeolites: Effect of Cation Type and Si/Al Ratio on Equilibrium and Kinetic Properties. *J. Langmuir* **2014**, *30*, 2968. [[CrossRef](#)]

**Disclaimer/Publisher's Note:** The statements, opinions and data contained in all publications are solely those of the individual author(s) and contributor(s) and not of MDPI and/or the editor(s). MDPI and/or the editor(s) disclaim responsibility for any injury to people or property resulting from any ideas, methods, instructions or products referred to in the content.